IEEE Access
Multidisciplinary | Rapid Review | Open Access Journal

SPECIAL SECTION ON KEY ENABLING TECHNOLOGIES FOR PROSUMER ENERGY MANAGEMENT

Received December 26, 2020, accepted January 9, 2021, date of publication January 13, 2021, date of current version January 26, 2021.

Digital Object Identifier 10.1109/ACCESS.2021.3051340

A Review of AC and DC Electric Springs

MINGHAO WANG[1], (Member, IEEE), YUFEI HE[1], (Member, IEEE), XU XU[1,2], (Member, IEEE), ZHEKANG DONG[3], (Member, IEEE), AND YU LEI[4]

[1]Department of Electrical Engineering, The Hong Kong Polytechnic University, Hong Kong, China
[2]School of Electrical and Electronic Engineering, Nanyang Technological University, Singapore 639798
[3]School of Electronics and Information, Hangzhou Dianzi University, Hangzhou 310018, China
[4]School of Automation, Wuhan University of Technology, Wuhan 430070, China

Corresponding author: Yu Lei (leiyu9087@whut.edu.cn)

This work was supported in part by the Hubei Provincial Natural Science Foundation of China under Grant 2020CFB549, in part by the National Natural Science Foundation of China under Grant 62001149, and in part by the Zhejiang Provincial Nature Science Foundation of China under Grant LQ21F010009.

ABSTRACT The large-scale integration of renewable energy sources in the power system can render instability issues, which degrades the power quality of the voltage supply. To address this issue, the electric springs (ES), which are elastic load demand control technologies, have been reported. Since it was proposed in 2011, many literatures on the applications, circuit topologies, control designs and the stability analysis of the ES have been reported. Based on the reported literatures, a comprehensive review of AC and DC ES technologies has been performed in this paper. The research outcomes are systematically summarized. The trend of the potential development of ES technologies is envisioned.

INDEX TERMS Demand-side management, electric springs, power system, smart grid.

I. INTRODUCTION

The utilization of renewable energy sources has been dramatically promoted by the energy crisis and environmental issues around the world during the past few decades [1]. Many European Union (EU) countries have targeted a share of 20% renewable energy sources in the final gross energy consumption by 2020 and increase the share to 27% by 2030 [2]. But sustainable integration of renewable energy sources, e.g., wind and solar, will inevitably pose great challenges to power system operation because of their intermittent power generation [3], [4]. Various solutions are proposed to tackle the instability issues arising from the integrated distributed renewable generations [5].

At the generation side, distributed generation systems can be aggregated as a virtual power plant (VPP) [6], [7] with higher power capacity, which offers a more reliable power supply than a single generation set through coordinating various generations. Microgrid [8], [9] is another effective solution. It is essentially a comprehensive integration of local renewable energy sources, loads and energy storage systems (ESS). The microgrids can exchange energy with the main grid in grid-connected mode and provide power to local loads in case of emergency in island mode. The control and operation strategies of microgrids are different from the conventional power system [10], [11]. It receives worldwide attention in the last few decades. Modern grid-supporting devices such as flexible alternating current transmission systems (FACTS), high voltage direct current transmission systems (HVDC) and energy storage system (ESS) are power electronics-based systems designed to improve the transmission controllability and capacity [12]–[15].

As an effective solution to buffer the fluctuating renewable generation, the energy storage systems, such as the batteries, flywheels and pumped storage power stations, are criticized for their relatively high cost and sluggish dynamic response. Demand-side management (DSM) [16]–[18] technology provides an alternative option that demands power consumption can be adaptively changed to follow the generation. Considering the difficulties in the control of clumsy bulk generation to follow the volatile distributed renewable generation, the DSM method is relatively more feasible for real-time implementation. This ''demand-following-generation'' method can lead to (i) reduced cost for load-demand balancing, (ii) improved efficiency of the grid, (iii) improved economy of real-time operation and (iv) enhanced power quality. Demand response can be implemented in many ways including direct load control, price-based programs and automated demand response

The associate editor coordinating the review of this manuscript and approving it for publication was Jiayong Li.

(ADR) [19]. Consumers can take actions to change their power consumption in response to signals (e.g., price information or power commands) sent by power grid operators. However, it is difficult to ensure a high response from the load side since consumers' comfort could be disrupted in the process.

The other DSM methods can be categorized into discrete and continuous types. For the discrete type, the load demands are remotely switched on and off by the system operator under a mutual agreement of subsidy and operation protocol. Such discrete control is achieved by using an active switch. Although the achievable load adjustment is either full load or no load, the aggregated control of massive loads can potentially achieve nearly-smooth granular load manipulation, which renders the minimum impacts to the power system [20]. However, the computation efforts and control complexity increase dramatically with the increase of the controllable loads, which is still a challenging issue for the real-time application. For the continuous DSM technology, the controllable loads are achieved by the switch-mode power converters [21]. The deferrable power quality of the interfaced load enables a deviation of the operating point away from the nominal values, which contributes to a dispatchable load profile for DSM. Typical applications can be the use of an adaptive heat pump [22], where the control of ambiance temperature is slack for achieving the elastic load control. Another generalized way of achieving continuous DSM is ES [23]. It is a first attempt to introduce the Hook's Law of mechanical spring to the electric system. A switch-mode voltage converter, which is termed as ES, is connected in series with a deferrable load. Such a configuration enables a smart load, whose load profile can be manipulated via the control of the ES output voltage. The ES-based smart load is massively distributed in the power system to perform the grid stabilization functionalities against the disturbance from the integrated renewables. Initially, the ES is proposed for stabilizing the voltages at the points of common coupling. With the addition of energy storage, another ancillary functions of frequency stabilization [24], three-phase balancing [25], storage reduction [26], harmonic cancellation [27] etc, have been achieved by using the ES. Besides the versatile functions of a three-phase or single-phase ES, the different control methods [28], collaborative control scheme [29] and dispatch strategies [30] have also been reported.

Since the proposal of the ES concept [23] in renewables-integrated AC grids, many research works have been performed on the control, circuit topology, application, etc. These research findings have covered different aspects of the ES application. To summarize the research achievements on the ES technology and envision the potential future development of ES, a comprehensive review of AC and DC ES is performed. Originated from the typical instability issues in AC and DC grids, the concept of different types of ES is revisited. The circuit topologies are summarized and compared. The control and application of single and multiple ES are summarized. Based on the current research achievements, the possible development of the ES technology is discussed.

II. INSTABILITY ISSUES INDUCED BY RENEWABLES

A. AC GRIDS

The equivalent circuit diagram and phasor diagram of a distribution line can be plotted as shown in Fig. 1(a) and 1(b). A power flow of P_s+jQ_s is transferred from the sending terminal s to the receiving portal. For the voltage polarities shown in Fig. 1(a), the voltage of the receiving terminal can be expressed as

$$|V_r|^2 = (|V_s| - \frac{P_s}{|V_s|}R - \frac{Q_s}{|V_s|}X)^2 + (\frac{Q_s}{|V_s|}R - \frac{P_s}{|V_s|}X)^2 \quad (1)$$

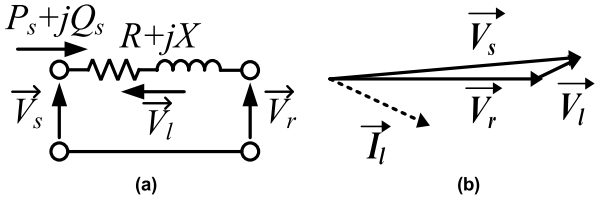

FIGURE 1. (a) Equivalent circuit diagram and (b) phasor diagram of a distribution line.

By neglecting the orthogonal term of $(\frac{Q_s}{|V_s|}R - \frac{P_s}{|V_s|}X)^2$, the voltage at the receiving terminal can be expressed as

$$|V_r| = |V_s| - \frac{P_s}{|V_s|}R - \frac{Q_s}{|V_s|}X \quad (2)$$

In the low voltage distribution network (LVDN), the line impedances are of considerable resistive component [31]. Considering the fluctuating active power generated by the distributed renewables and V_s is tightly regulated at the substation, the voltages at the receiving end will fluctuate with respect to the volatile generation of the interfaced renewables. Considering the non-negligible inertia of the rotor, the simplified power balance in a renewables-integrated power system can be expressed as

$$P_s + P_r = P_L + J_r\omega_f \frac{d\omega_f}{dt} \quad (3)$$

where J_r is the rotational inertia of the rotor, ω_f is the angular speed of the rotor. P_S, P_L and P_r denote the source power, load power and renewable power, respectively. Considering the dynamic response of the bulk generation is slow, the volatile renewable generation will be buffered by the kinetic energy stored in the rotor. Since the grid frequency f is anchored with the rotating speed of the synchronous generator, the changing rotating speed of the rotor will lead to the frequency fluctuation of the grid frequency, which jeopardizes the grid stability.

Besides, the occasional faults, which can initiate the low voltage protection of the connected renewable generations, can also render the frequency instability of the grid. When the unexpected low grid voltage induced by faults activates the disconnection of renewables, the instantaneous loss of active

power generation must be provided via the deceleration of the rotor, which undermines the grid frequency stability.

B. DC GRIDS

In DC grids, the connected appliances are generally converter interfaced. The capacitors are installed at the DC bus for reducing the switching ripples and providing relatively smooth DC voltages for the appliances. The power balance at a DC bus can be expressed as

$$P_s + P_r = P_L + C_M v_M \frac{dv_M}{dt} \tag{4}$$

where v_M and C_M are the DC mains voltage and equivalent DC capacitance, respectively. As shown in (4), the variation of P_r will render the charging and discharging of C_M, which makes the bus voltage to fluctuate. Similarly, the integration of single-phase power conversion systems and occasional faults can also lead to the change of V_{bus}. Correspondingly, double-line-frequency harmonics [32] and flickers will be generated on V_M.

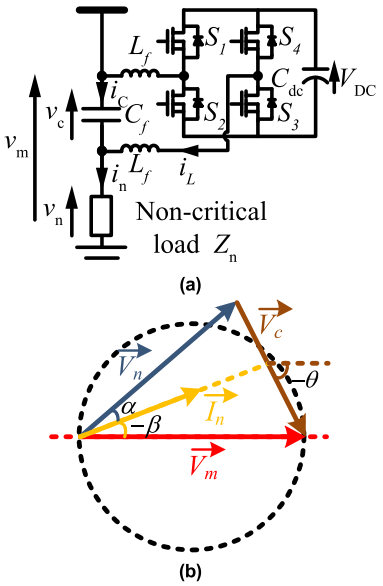

FIGURE 2. (a) Equivalent circuit diagram and (b) phasor diagram of ES-1 based smart load [33].

III. CONCEPTS AND BASIC OPERATING PRINCIPLES OF AC AND DC ES

A. AC ES

The concept of the electric spring is firstly reported in [23]. Following the concept of mechanical springs, a controllable voltage source, which is achieved by switch-mode power converters, is serially connected with a non-critical load (NCL), which is deferrable load with relatively-large tolerance of its applied voltage. This controllable voltage, which is termed as electric spring, generates a controllable voltage profile for shaping the power flow of this branch. In this way, the branch power will follow the pattern of the intermittent generation in a real-time matter and the smart load function can be achieved. The circuit schematic diagram of the ES based smart load can be plotted as shown in Fig. 2(a). The corresponding phasor diagram can be plotted as shown in Fig. 2(b).

The first generation of electric spring (ES-1) uses a DC-link capacitor as its energy storage and the ES-1 adopts reactive-power-controlled active power compensation. As shown in Fig. 2(b), since the ES-1 cannot store or deliver active power, the load current $\vec{I}_n$ must be perpendicular to the ES voltage $\vec{V}_c$. For the simplification of analysis, the NCL is considered as purely resistive, i.e., $Z_n = R_n$. When the bus voltage $\vec{V}_m$ is regulated to the reference, the power balance between the power sources and demands is shown in (3) can be rewritten as

$$P_s + P_r = P_L + J_r \omega_f \frac{d\omega_f}{dt} = \frac{|V_m|^2 - |V_c|^2}{R_n} + J_r \omega_f \frac{d\omega_f}{dt} \tag{5}$$

In (5), P_L is adaptively changed so that the load demand will follow the intermittent profile of P_r. The volatile renewable generation is therefore compensated. For the ES-1 based smart load, the compulsory orthogonal relation between $\vec{I}_n$ and $\vec{V}_c$ will lead to a coupled relationship between the smart load active power P_L and reactive power Q_L. This renders a singular functionality of ES-1, i.e., the ES-1 cannot perform frequency stabilization and voltage regulation concurrently.

The second generation of ES (ES-2) is imbedded with DC-link energy storage devices. The ES-2 can achieve four-quadrant operations. The general steady-state analysis is performed in [34]. By referring to Fig. 2(b), the powers of the ES and the smart load can be calculated as

$$\begin{cases} P_c = \dfrac{|V_m||V_c|\cos(\alpha-\theta) - |V_c||V_c|\cos\alpha}{|Z_n|} \\ Q_c = \dfrac{|V_m||V_c|\sin(\alpha-\theta) - |V_c||V_c|\sin\alpha}{|Z_n|} \\ P_L = \dfrac{|V_m||V_m|\cos\alpha - |V_m||V_c|\cos(\theta+\alpha)}{|Z_n|} \\ Q_L = \dfrac{|V_m||V_m|\sin\alpha - |V_m||V_c|\sin(\theta+\alpha)}{|Z_n|} \end{cases} \tag{6}$$

By referring to (6), the basic operating modes of ES-1 and E-2 can be summarized in Table 1 of the Appendix.

As illustrated in Table 1 of the Appendix, the ES-2 can achieve the decoupled control of its active and reactive power, which leads to a wider power compensation ability.

By the circuit duality, the shunt type ES can be configured as a controllable current source, which can be achieved by using the grid-tied power converter [35]. The function of shunt ES is very similar to the STATCOM and grid-connected storage systems. Similarly, with the capacitive DC-link storage, the shunt ES can achieve two-quadrant reactive power compensation. When the energy storage devices are installed in the shunt ES, a four-quadrant power compensation can be achieved. It is worthy of mentioning that the shunt ES is different from STATCOM and grid-connected storage systems in terms of capacity and allocation. Since the shunt ES is

applied at the distribution grid, they are of small capacity and massively distributed in the grid.

B. DC ES

The distinct advantages of ES are not only possessed in the AC power system but also maintained when the concept of ES is extended to the DC distribution network. Research works exploring the voltage stability, power quality improvement and energy storage reduction are being conducted with DC Electric Spring (DC ES). Similar to AC ES, DC ES also has different configurations, namely, series and shunt ES.

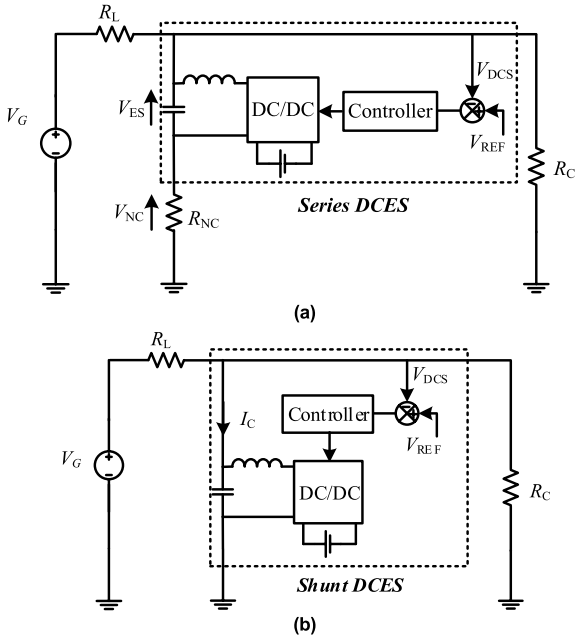

FIGURE 3. Equivalent circuit diagrams of DC ES (a) series type and (b) shunt type.

The concept of the DC ES is firstly reported in [36], [37]. The simplified circuit diagram of the DC ES can be plotted as shown in Fig. 3. The series DC ES is essentially a controllable DC voltage source, while the shunt DC ES is a controllable current source. For the series DC ES, it outputs a tunable voltage source so that the applied DC voltage of the NCL will be changed. For the shunt DC ES, it delivers a controllable current to the grid and does not associate with any NCL. The general steady-state analysis of the series DC ES is performed in [36] and a comprehensive comparative study of the series and shunt DC ES is reported in [37].

As shown in Fig. 3(a), batteries are installed at the DC link of the series DC ES to exchange power with the converter and LC filter at the output side. The series DC ES is integrated with DC noncritical load (NCL) and forms a DC smart load (SL).

With controllable output voltage V_C, series DC ES can change the power consumption of NCL and SL to regulate the DC mains voltage V_M. Take a positive-resistive NCL as an example, the relationship among the ES voltage V_C, load voltage V_{NC} and bus voltage V_M can be expressed as

$$V_M = V_C + V_{NC} \tag{7}$$

Correspondingly, the powers of the series DC ES and the SL can be expressed as

$$\begin{cases} P_C = \dfrac{V_C(V_M - V_C)}{R_{NC}} \\ P_L = \dfrac{V_M(V_M - V_C)}{R_{NC}} \end{cases} \tag{8}$$

By substituting (8) into (4), it can be derived that

$$P_s + P_r = P_L + C_M v_M \frac{dv_M}{dt} = \frac{V_M(V_M - V_C)}{R_{NC}} + C_M v_M \frac{dv_M}{dt} \tag{9}$$

As shown in (9), when V_M is regulated to the reference, the fluctuating part of P_r will be consumed by P_L and the deviation of DC mains voltage $\frac{dv_M}{dt}$ will be 0.

Since the shunt DC ES is tied to mains, its voltage V_C always equals to bus voltage V_M. Therefore, its voltage and power can be calculated by using

$$\begin{cases} V_C = V_M \\ P_L = V_M I_C \end{cases} \tag{10}$$

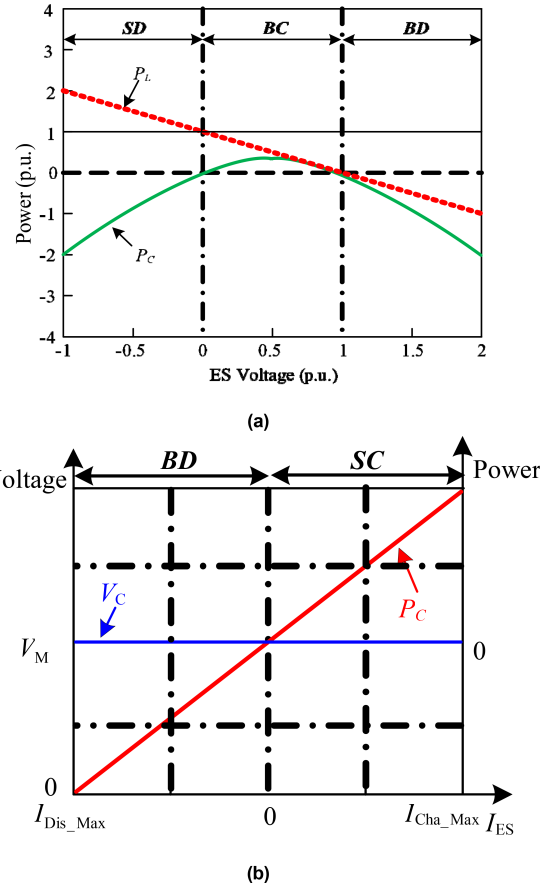

FIGURE 4. Voltage-current operating curves of DC ES (a) series type and (b) shunt type.

The operating curves of the series and shunt DC ES can be plotted as shown in Fig. 4. Judging from whether the DC ES

battery is charging or discharging, and the DC mains voltage is boosted or suppressed, four operating modes of the series and shunt DC ES can be achieved, i.e.,

- Boosting & discharging mode (BD);
- Boosting & charging mode (BC);
- Suppressing & discharging mode (SD);
- Suppressing & charging mode (SC).

These modes can be summarized as shown in Table 2 of the Appendix.

IV. CIRCUIT TOPOLOGIES OF AC AND DC ES

A. AC ES CONVERTERS

Based on the previous analysis, the AC ES, both the series and shunt types, require bipolar voltage output and bidirectional power flow. The conventional inverters are applicable as the AC ES. According to the reported works about the AC ES, the features of different types of ES circuit topologies are summarized as shown in Table 3 of the Appendix.

It is worthy of mentioning that the topologies 3, 4 and 5 are essentially a hybrid topology of series and shunt AC ES. These circuits have three terminals, namely, grid, NCL and the ground. They can be operated either as a series ES or a shunt ES. As discussed in [26], the achievable power compensation region of a series and a shunt AC ES can be plotted as shown in Fig. 5.

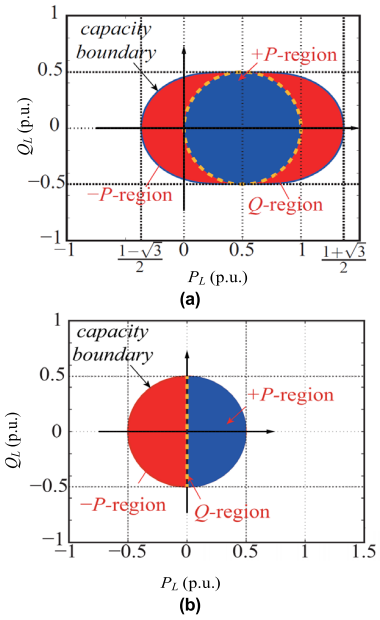

FIGURE 5. Active and reactive power compensation region of (a) series type and (b) shunt type ACES in per-unit system [26].

Therefore, the achievable active and reactive power compensation regions of the hybrid structure are the sum of Fig. 5(a) and 5(b).

B. DC ES CONVERTERS

Different from the AC ES, the series and shunt DC ES have different requirements on the applied power converters. Both the series and shunt DC ES require the energy storage, e.g., batteries, for achieving the load adjustment. For the series ES, similar to its AC counterpart, it requires bipolar voltage output and bidirectional power flows. Therefore, the converters, which are applicable as series AC ES, can be applied as series DC ES. For the shunt DC ES, it requires unipolar voltage output and bidirectional power flow. The typical circuit topologies for DC ES application can be summarized as shown in Table 4 of the Appendix.

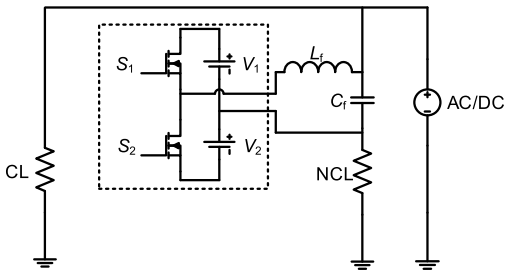

FIGURE 6. Illustration of a half-bridge converter being applied as a series AC and DC ES.

It is worthy of mentioning that the DC power is different from the AC power. In steady-state, the AC power of the positive-half cycle is nearly identical to that of the negative cycle. For the half-bridge converter shown in Fig. 6, although the inevitable power differences between the positive and negative cycle will render the unbalanced DC link capacitor voltage, the use of voltage balancing control loop can address this issue.

However, in the DC system, the power of the upper and lower batteries will never be balanced without intervening in the operation of the DC ES. By denoting D, T_s and V_B as the duty ratio of S_1, switching period and the battery voltage. The ES voltage and the battery powers can be calculated as

$$\begin{cases} V_C = (2D-1)V_B \\ \dfrac{P_1}{P_2} = \dfrac{D}{D-1} \end{cases} \tag{11}$$

By (11), when the output voltage V_C is changed, the power of the upper and lower batteries will be different, which leads to the unbalanced operation of DC-link batteries. A simulation is performed to demonstrate the upper and lower battery energies for different operating modes of the series DC ES.

As can be seen from Fig. 7, with respect to the BD, BC and SD operating modes, the DC ES battery power will be different. The sum of the upper and lower battery power profile is nearly the same with the full-bridge converter battery power. In BD mode ($D \gg 0.5$ and $I_L < 0$), the upper battery discharges to power the grid, while the lower battery is charged up. However, due to the shedding of NCL, the charging current I_L is not large. In BC mode ($D > 0.5$ and $I_L > 0$), the upper battery charges more energy than the energy discharged by the lower battery. In SD mode ($D < 0.5$ and $I_L >$ nominal NCL current), the lower battery discharges a lot of energy, while the upper battery charges some energy. The overall effect results in the upper battery being fully charged easily while the lower battery is drained out.

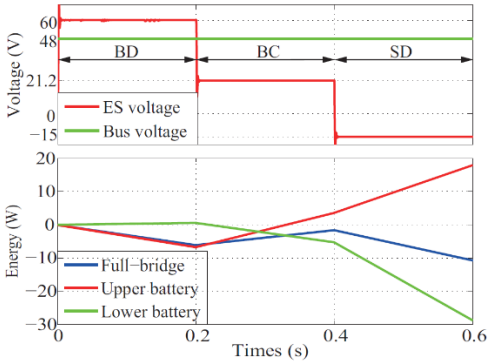

FIGURE 7. Simulated waveforms of using a half-bridge and a full-bridge converter as series ES.

As the DC ES is required to perform bus voltage regulation and harmonic filtering, both the harmonic power and DC power will be buffered by the storages of DC ES. In terms of different energy storages, the capacitive storage is preferable for buffering the regenerative harmonic power and the battery storage is feasible to handle the unbalanced DC power. The coupling of harmonic power and DC power can lead to the reduced battery lifetime of the battery. A similar issue also exists in the single-phase system (e.g. single-phase inverter and rectifier) and many active power decoupling methods have been reported to diver the AC harmonic power from the DC terminal to capacitive and inductive storage devices [43]. For the DC ES, a hybrid structure, which consists of a shunt half-bridge converter and serial full-bridge converter as shown in Fig. 8, is reported in [42] for the concurrent operation of harmonic filtering and voltage regulation.

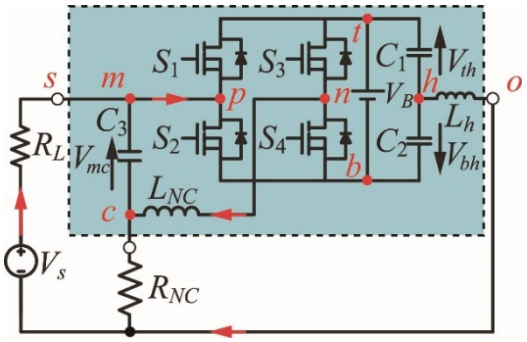

FIGURE 8. The half-bridge and full-bridge hybrid structure for DC ES application [42].

With the power decoupling control, the embedded shunt half-bridge converter, which consists of branch *P* and DC-link capacitors, can divert the harmonic power into C_1 and C_2. In the meantime, the full-bridge converter, which is comprised of branches *P, n,* and battery V_B, will be used to manipulate the load current I_L.

V. APPLICATION AND CONTROL OF ES

In the previous sections, the operating principles and circuit topologies of AC and DC ES are summarized. Based on the different characteristics of the different types of circuit topologies, the ES can perform different functions. In this section, the applications of the AC and DC ES will be summarized. The corresponding control schemes are also discussed.

A. AC ES

Since the ES-based smart load can adjust the demand side active and reactive powers, they can be used for the grid frequency and voltage regulation. In [44], the ''input-feedback-input-control'' scheme is reported to control the ES-1 voltage for regulating the bus voltage. As shown in Fig. 9(a), the root-mean-square value of the bus voltage is used as the feedback to generate the amplitude control signal of the ES voltage. It is considered that the voltage amplitude of ES-1 is positively associated with the generated reactive power (i.e., the capacitive reactive power) of the smart load. The voltage compensation effects between the ES-1 and the STATCOM are compared in [45]. However, the NCL will affect the operating regime of the ES and the dynamic response of the smart load. To improve the performance and the reliability of the ES-1 based smart load in the bus voltage regulation, the smart load steady-state operation mode is used to derive the voltage reference of ES-1 in [33]. When the battery storage is added, the ES-2 can perform the decoupled control of the smart load active and reactive power [46]. In [47], the *dq* rotating frame-based control strategy is reported, as shown in Fig. 9(b), to decouple the harmonic filtering operation and the control of ES voltage. To achieve the accurate steady-state regulation of the bus voltage, a δ-control scheme is reported in [48]. Compared with the previous two methods, the δ-control demands many measurements and system information. To further decouple the control of the smart load active and reactive, a radial-chordal decomposition (RCD) control scheme is proposed in [49]. In this control scheme, the ES voltage is decomposed with respect to the NCL voltage. By adjusting the radial component of the ES voltage, the applied voltage amplitude of the NCL will be changed. By adjusting the chordal component of the ES voltage, the phase angle of the NCL voltage will be changed. In this way, the control of the power factor and the load current amplitude can be decoupled.

In [47], the ES-2 based smart load is used to performing harmonic filtering. Equivalently, the ES-2 can be considered as a negative impedance connected in series with the NCL. With the proportional-resonant controller, the overall equivalent impedance of the smart load at the harmonic frequency can be set at 0 so that the harmonic current can be diverted to the smart load. However, the ES-2 has to provide extra power to perform the harmonic filtering operation.

To assist the integrated renewable generation to perform the low-voltage-ride-through (LVRT) operation, the reactive power is required to be injected immediately for supporting the grid voltage and avoiding the tripping of renewables. In [50], the reactive power compensating ability of the back-to-back ES is exploited and optimized for

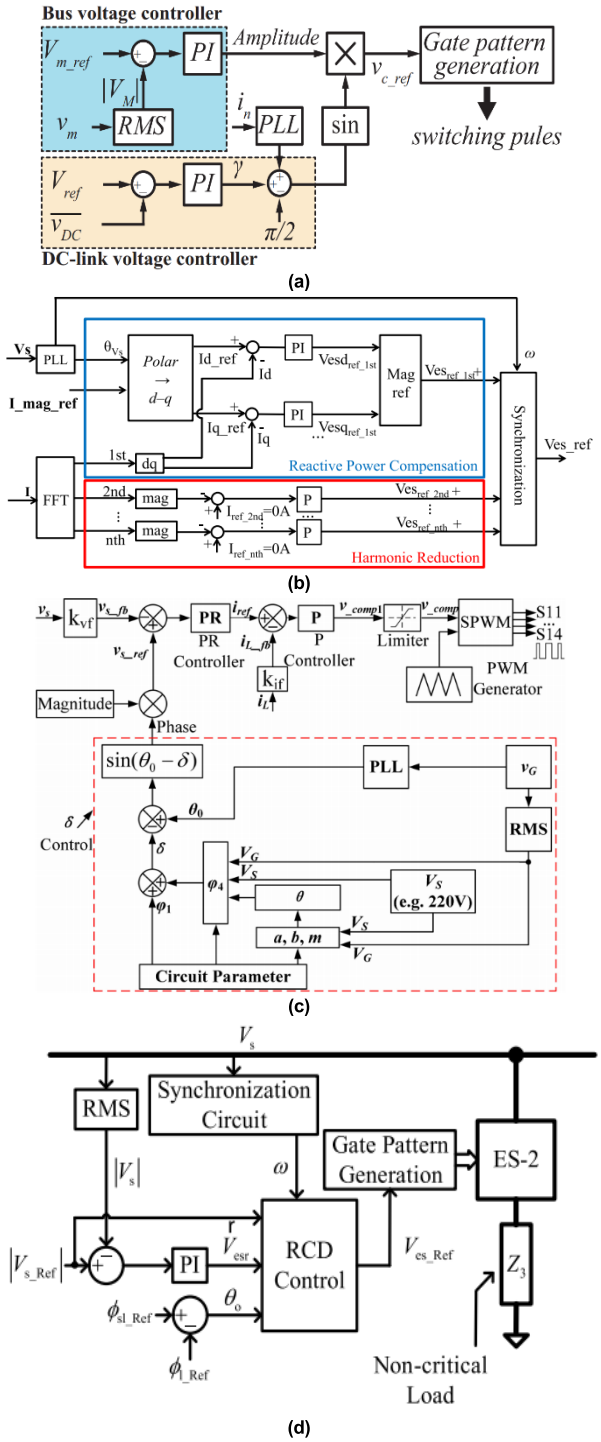

FIGURE 9. Control block diagrams of (a) input-feedback-input-control [44], (b) dq rotating frame-based control [47] (c) δ control [48] and (d) RCD control [49].

injecting the maximum available reactive power to the grid.

For the three-phase system, the three-phase imbalance issue is a threat to both the grid and the load. In [25], the three-phase ES-2 is reported to balance the three-phase voltage. Since the three-phase ES will be used to process unbalanced three-phase power. The instantaneous power theory is applied to the control of three-phase ES to derive the optimal three-phase voltage references so that the pulsating power at the DC terminal can be minimized [51].

Although the ESs are of small power capacity, they are massively distributed in the system. For the coordination of multiple ESs, the droop control is reported in [52] to achieve the reactive power sharing among multiple ES-1. In the droop control scheme, the steady-state regulation is sacrificed for achieving reactive power sharing. To remedy this drawback, the consensus control scheme, which uses the limited communication network, is reported in [53]. The consensus controller can operate the ES voltage towards a consensus averaged value, which will unavoidably lead to the task sharing among many different devices.

B. DC ES

The application of the DC ES on addressing the (i) bus voltage variation, (ii) harmonic contamination and (iii) voltage flickers have been elaborated in [37]. These applications can be illustrated as shown in Fig. 10.

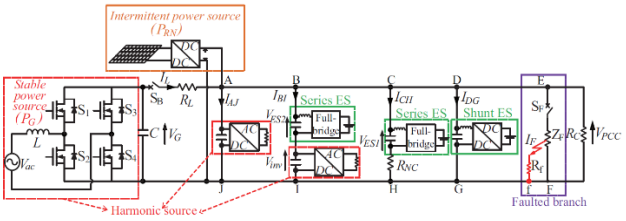

FIGURE 10. A DC grid integrated with series and shunt DC ES.

The performances of series and shunt DC ES in performing (i) bus voltage regulation, (ii) harmonic filtering and (iii) LVRT can be summarized as shown in Table 5 of the Appendix. For the bus voltage regulation, the series DC ES can manipulate the power profile of the NCL while the shunt DC ES cannot. This renders that the required energy storage capacity of the series DC ES for balancing the generation and demand can be smaller than that of the shunt DC ES. As for performing the harmonic filtering, the series ES has to generate negative voltage so that the smart load branch can have a nearly-zero impedance at the harmonic frequency. This requires extra power dissipation on the NCL. As the shunt DC ES interacts with the DC system directly, it does not have this issue. For the LVRT performance, since the shunt DC ES can directly provide currents to the grid, it can achieve a faster dynamic response than the series DC ES.

For the application of multiple ES, the droop-based decentralized control scheme is reported in [54] for the series DC ES. Since the differently rated NCL can affect the power of the series DC ES batteries, the objective of minimization

TABLE 1. Operating modes of ES-1 and ES-2.

Mode/Type	Inductive	Capacitive	Resistive	Resistive & inductive	Resistive & capacitive	Negatively Resistive & inductive	Negatively Resistive & capacitive
ES-1	$P_c = 0$ $Q_c > 0$	$P_c = 0$ $Q_c < 0$	NA	NA	NA	NA	NA
ES-2	$P_c = 0$ $Q_c > 0$	$P_c = 0$ $Q_c < 0$	$P_c > 0$ $Q_c = 0$	$P_c > 0$ $Q_c > 0$	$P_c > 0$ $Q_c < 0$	$P_c < 0$ $Q_c > 0$	$P_c < 0$ $Q_c < 0$

TABLE 2. Operating modes of series and shunt DC ES.

Mode/Type	Boosting & Discharging	Boosting & Charging	Suppressing & Discharging	Suppressing & Charging
Series DC ES	$V_C > V_M$ $P_C < 0$	$0 < V_C < V_M$ $P_C > 0$	$V_C < 0$ $P_C < 0$	NA
Shunt DC ES	$I_C < 0$ $P_C < 0$	NA	NA	$I_C > 0$ $P_C > 0$

TABLE 3. Different circuit topologies for AC ES application.

No.	Topology	Isolation	Operating range		Required active switches	Circuit complexity	DC-link voltage balancing
			Without large energy storage	With large energy storage			
1	Half-bridge[23]	Non-isolated	Small	Medium	2	Simple	Required
2	Full-bridge[33]	Non-isolated	Small	Medium	4	Simple	Not required
3	Back-to-back [38]	Isolated	Medium	Large	4	Complicated	Required
4	Full-bridge with split DC link [26] [39]	Non-isolated	Medium	Large	4	Simple	Required
5	Three-phase full-bridge [40]	Non-isolated	Medium	Large	6	Simple	Not required
6	Full-bridge + Serially-connected transformer [41]	Isolated	Small	Medium	4	Complicated	Not required
7	Multi-port magnetically-coupled [33]	Isolated	Small	Medium	4	Complicated	Not required

charging and discharging battery power can be programmed in the design of the droop controller. The other reported works on the DC ES generally focus on the control and application of DC ES in the unipolar DC grid. Typically, the concurrent regulation of nodal voltages and the battery states of charge (SoC). In [55], the consensus control is applied to equalize the battery SoC and regulate the bus voltage to the reference simultaneously.

Besides the unipolar DC microgrid, the series ES is also reported in [56] for balancing the voltages in bipolar DC grids. A decoupling controller is designed in [56] to operate two series DC ES in a decoupled way for reducing the neutral current and restoring the voltages.

VI. CONCLUSION

The electric springs are an effective demand-side management technology for taming the intermittency of the renewables. In this paper, the operating principle, circuit topology, application and control methods of the AC and DC electric springs are summarized. The reported research works have developed all kinds of functionalities of the ES hardware. As the ES is a distributed DSM mechanism, the coordination of multiple ES in DC and AC grids still requires further investigation.

APPENDIX

Five tables are presented below.

TABLE 4. Different circuit topologies for series and shunt DC ES application.

No.	Topology	Isolation	Achievable operating modes				Required active switches	Battery power
			BD	BC	SD	SC		
1	Half-bridge [36]	Non-isolated	√	√	√	×	2	Unbalanced and coupled
2	Full-bridge [37]	Non-isolated	√	√	√	×	4	Balanced and coupled
3	Full-bridge with split DC link [42]	Non-isolated	√	√	√	×	4	Balanced and decoupled
4	Watkins-Johnson	Non-isolated	√	√	√	×	4	Balanced and coupled
5	Push-Pull	Isolated	√	√	√	×	2	Balanced and coupled
6	Synchronous buck	Non-isolated	√	×	×	√	2	Balanced and coupled
7	Bidirectional buck-boost	Non-isolated	√	×	×	√	2	Balanced and coupled

TABLE 5. Performance comparison between series and shunt DC ES.

	Bus voltage regulation	Harmonic filtering	LVRT
Series DC ES	Automatic NCL manipulation	Require power dissipation on NCL	Slow dynamic response
Shunt ES	Independent of NCL	Independent of NCL	Fast dynamic response

ACKNOWLEDGMENT

(Minghao Wang and Yufei He contributed equally to this work.)

REFERENCES

[1] J. Li, C. Liu, M. Khodayar, M. Wang, Z. Xu, B. Zhou, and C. Li, "Distributed online VAR control for unbalanced distribution networks with photovoltaic generation," *IEEE Trans. Smart Grid*, vol. 11, no. 6, pp. 4760–4772, Nov. 2020.

[2] Eurostat, Press, and Office. (2017). *Eleven EU Countries Hit 2020 Renewable Energy Targets*. [Online]. Available: https://ec.europa.eu/energy/en/news/eleven-eu-countries-hit-2020-renewable-energy-targets

[3] E. J. Coster, J. M. A. Myrzik, B. Kruimer, and W. L. Kling, "Integration issues of distributed generation in distribution grids," *Proc. IEEE*, vol. 99, no. 1, pp. 28–39, Jan. 2011.

[4] J. Li, C. Zhang, Z. Xu, J. Wang, J. Zhao, and Y.-J.-A. Zhang, "Distributed transactive energy trading framework in distribution networks," *IEEE Trans. Power Syst.*, vol. 33, no. 6, pp. 7215–7227, Nov. 2018.

[5] J. Li, Z. Xu, J. Zhao, and C. Zhang, "Distributed online voltage control in active distribution networks considering PV curtailment," *IEEE Trans. Ind. Informat.*, vol. 15, no. 10, pp. 5519–5530, Oct. 2019.

[6] G. Zhang, C. Jiang, and X. Wang, "Comprehensive review on structure and operation of virtual power plant in electrical system," *IET Gener., Transmiss. Distrib.*, vol. 13, no. 2, pp. 145–156, Jan. 2019.

[7] H. Saboori, M. Mohammadi, and R. Taghe, "Virtual power plant (VPP), definition, concept, components and types," in *Proc. Asia–Pacific Power Energy Eng. Conf.*, Mar. 2011, pp. 1–4.

[8] X. Yu, C. Cecati, T. Dillon, and M. Simões, "The new frontier of smart grids," *IEEE Ind. Electron. Mag.*, vol. 5, no. 3, pp. 49–63, Sep. 2011.

[9] F. Katiraei, R. Iravani, N. Hatziargyriou, and A. Dimeas, "Microgrids management," *IEEE Power Energy Mag.*, vol. 6, no. 3, pp. 54–65, May/Jun. 2008.

[10] J. M. Guerrero, J. C. Vasquez, J. Matas, L. García de Vicuna, and M. Castilla, "Hierarchical control of droop-controlled AC and DC microgrids—A general approach toward standardization," *IEEE Trans. Ind. Electron.*, vol. 58, no. 1, pp. 158–172, Jan. 2011.

[11] J. Rocabert, A. Luna, F. Blaabjerg, and P. Rodríguez, "Control of power converters in AC microgrids," *IEEE Trans. Power Electron.*, vol. 27, no. 11, pp. 4734–4749, Nov. 2012.

[12] F. Z. Peng, "Flexible AC transmission systems (FACTS) and resilient AC distribution systems (RACDS) in smart grid," *Proc. IEEE*, vol. 105, no. 11, pp. 2099–2115, Nov. 2017.

[13] N. Flourentzou, V. G. Agelidis, and G. D. Demetriades, "VSC-based HVDC power transmission systems: An overview," *IEEE Trans. Power Electron.*, vol. 24, no. 3, pp. 592–602, Mar. 2009.

[14] B. P. Roberts and C. Sandberg, "The role of energy storage in development of smart grids," *Proc. IEEE*, vol. 99, no. 6, pp. 1139–1144, Jun. 2011.

[15] M. G. Molina, "Energy storage and power electronics technologies: A strong combination to empower the transformation to the smart grid," *Proc. IEEE*, vol. 105, no. 11, pp. 2191–2219, Nov. 2017.

[16] T. Samad, E. Koch, and P. Stluka, "Automated demand response for smart buildings and microgrids: The state of the practice and research challenges," *Proc. IEEE*, vol. 104, no. 4, pp. 726–744, Apr. 2016.

[17] A. Brooks, E. Lu, D. Reicher, C. Spirakis, and B. Weihl, "Demand dispatch," *IEEE Power Energy Mag.*, vol. 8, no. 3, pp. 20–29, May/Jun. 2010.

[18] D. S. Callaway and I. A. Hiskens, "Achieving controllability of electric loads," *Proc. IEEE*, vol. 99, no. 1, pp. 184–199, Jan. 2011.

[19] J. S. Vardakas, N. Zorba, and C. V. Verikoukis, "A survey on demand response programs in smart grids: Pricing methods and optimization algorithms," *IEEE Commun. Surveys Tuts.*, vol. 17, no. 1, pp. 152–178, 1st Quart., 2015.

[20] Z. Xu, J. Ostergaard, and M. Togeby, "Demand as frequency controlled reserve," *IEEE Trans. Power Syst.*, vol. 26, no. 3, pp. 1062–1071, Aug. 2011.

[21] L. Yang, N. Tai, C. Fan, and Y. Meng, "Energy regulating and fluctuation stabilizing by air source heat pump and battery energy storage system in microgrid," *Renew. Energy*, vol. 95, pp. 202–212, Sep. 2016.

[22] S. Kawachi, J. Baba, and H. Hagiwara, "Energy capacity reduction of energy storage system in microgrid by use of heat pump: Characteristic study by use of actual machine," in *Proc. 14th Int. Power Electron. Motion Control Conf.*, Sep. 2010, pp. T11–52.

[23] S. Y. Hui, C. K. Lee, and F. F. Wu, "Electric springs—A new smart grid technology," *IEEE Trans. Smart Grid*, vol. 3, no. 3, pp. 1552–1561, Sep. 2012.

[24] Q. Wang, M. Cheng, Y. Jiang, W. Zuo, and G. Buja, "A simple active and reactive power control for applications of single-phase electric springs," *IEEE Trans. Ind. Electron.*, vol. 65, no. 8, pp. 6291–6300, Aug. 2018.

[25] S. Yan, S.-C. Tan, C.-K. Lee, B. Chaudhuri, and S. Y. R. Hui, "Electric springs for reducing power imbalance in three-phase power systems," *IEEE Trans. Power Electron.*, vol. 30, no. 7, pp. 3601–3609, Jul. 2015.

[26] M.-H. Wang, T.-B. Yang, S.-C. Tan, and S. Y. Hui, "Hybrid electric springs for grid-tied power control and storage reduction in AC microgrids," *IEEE Trans. Power Electron.*, vol. 34, no. 4, pp. 3214–3225, Apr. 2019.

[27] Y. Shuo, S.-C. Tan, C. K. Lee, and S. Y. R. Hui, "Electric spring for power quality improvement," in *Proc. IEEE Appl. Power Electron. Conf. Expo. (APEC)*, Mar. 2014, pp. 2140–2147.

[28] T. Yang, T. Liu, J. Chen, S. Yan, and S. Y. R. Hui, "Dynamic modular modeling of smart loads associated with electric springs and control," *IEEE Trans. Power Electron.*, vol. 33, no. 12, pp. 10071–10085, Dec. 2018.

[29] J. Chen, S. Yan, T. Yang, S.-C. Tan, and S. Y. Hui, "Practical evaluation of droop and consensus control of distributed electric springs for both voltage and frequency regulation in microgrid," *IEEE Trans. Power Electron.*, vol. 34, no. 7, pp. 6947–6959, Jul. 2019.

[30] L. Liang, Y. Hou, and D. J. Hill, "An interconnected microgrids-based transactive energy system with multiple electric springs," *IEEE Trans. Smart Grid*, vol. 11, no. 1, pp. 184–193, Jan. 2020.

[31] M. S. Golsorkhi, Q. Shafiee, D. D.-C. Lu, and J. M. Guerrero, "Distributed control of low-voltage resistive AC microgrids," *IEEE Trans. Energy Convers.*, vol. 34, no. 2, pp. 573–584, Jun. 2019.

[32] P. T. Krein, R. S. Balog, and M. Mirjafari, "Minimum energy and capacitance requirements for single-phase inverters and rectifiers using a ripple port," *IEEE Trans. Power Electron.*, vol. 27, no. 11, pp. 4690–4698, Nov. 2012.

[33] M.-H. Wang, Y. He, T. Yang, Y. Jia, and Z. Xu, "Cascaded voltage control for electric springs with DC-link film capacitors," *IEEE J. Emerg. Sel. Topics Power Electron.*, vol. 8, no. 4, pp. 3982–3994, Dec. 2020.

[34] S.-C. Tan, C. K. Lee, and S. Y. Hui, "General steady-state analysis and control principle of electric springs with active and reactive power compensations," *IEEE Trans. Power Electron.*, vol. 28, no. 8, pp. 3958–3969, Aug. 2013.

[35] T. Yang, K.-T. Mok, S.-C. Tan, C. Kwan Lee, and S. Yuen Hui, "Electric springs with coordinated battery management for reducing voltage and frequency fluctuations in microgrids," *IEEE Trans. Smart Grid*, vol. 9, no. 3, pp. 1943–1952, May 2018.

[36] K. Mok, M. Wang, S. Tan, and S. Y. R. Hui, "DC electric springs—A technology for stabilizing DC power distribution systems," *IEEE Trans. Power Electron.*, vol. 32, no. 2, pp. 1088–1105, Feb. 2017.

[37] M.-H. Wang, K.-T. Mok, S.-C. Tan, and S. Y. Hui, "Multifunctional DC electric springs for improving voltage quality of DC grids," *IEEE Trans. Smart Grid*, vol. 9, no. 3, pp. 2248–2258, May 2018.

[38] S. Yan, C.-K. Lee, T. Yang, K.-T. Mok, S.-C. Tan, B. Chaudhuri, and S. Y. R. Hui, "Extending the operating range of electric spring using back-to-back converter: Hardware implementation and control," *IEEE Trans. Power Electron.*, vol. 32, no. 7, pp. 5171–5179, Jul. 2017.

[39] Y. Qi, T. Yang, J. Fang, Y. Tang, K. R. R. Potti, and K. Rajashekara, "Grid inertia support enabled by smart loads," *IEEE Trans. Power Electron.*, vol. 36, no. 1, pp. 947–957, Jan. 2021.

[40] H. Liu, W. M. Ng, C.-K. Lee, and S. Y. Ron Hui, "Integration of flexible loads and electric spring using a three-phase inverter," *IEEE Trans. Power Electron.*, vol. 35, no. 8, pp. 8013–8024, Aug. 2020.

[41] Q. Wang, M. Cheng, Z. Chen, and G. Buja, "A novel topology and its control of single-phase electric springs," in *Proc. Int. Conf. Renew. Energy Res. Appl. (ICRERA)*, Nov. 2015, pp. 267–272.

[42] M.-H. Wang, S. Yan, S.-C. Tan, and S. Y. Hui, "Hybrid-DC electric springs for DC voltage regulation and harmonic cancellation in DC microgrids," *IEEE Trans. Power Electron.*, vol. 33, no. 2, pp. 1167–1177, Feb. 2018.

[43] Y. Sun, Y. Liu, M. Su, W. Xiong, and J. Yang, "Review of active power decoupling topologies in single-phase systems," *IEEE Trans. Power Electron.*, vol. 31, no. 7, pp. 4778–4794, Jul. 2016.

[44] C. K. Lee, B. Chaudhuri, and S. Y. Hui, "Hardware and control implementation of electric springs for stabilizing future smart grid with intermittent renewable energy sources," *IEEE J. Emerg. Sel. Topics Power Electron.*, vol. 1, no. 1, pp. 18–27, Mar. 2013.

[45] X. Luo, Z. Akhtar, C. K. Lee, B. Chaudhuri, S.-C. Tan, and S. Y. R. Hui, "Distributed voltage control with electric springs: Comparison with STATCOM," *IEEE Trans. Smart Grid*, vol. 6, no. 1, pp. 209–219, Jan. 2015.

[46] X. Chen, Y. Hou, S.-C. Tan, C.-K. Lee, and S. Y. R. Hui, "Mitigating voltage and frequency fluctuation in microgrids using electric springs," *IEEE Trans. Smart Grid*, vol. 6, no. 2, pp. 508–515, Mar. 2015.

[47] S. Yan, S.-C. Tan, C.-K. Lee, B. Chaudhuri, and S. Y. R. Hui, "Use of smart loads for power quality improvement," *IEEE J. Emerg. Sel. Topics Power Electron.*, vol. 5, no. 1, pp. 504–512, Mar. 2017.

[48] W. Qingsong, C. Ming, C. Zhe, and W. Zheng, "Steady-state analysis of electric springs with a novel δ control," *IEEE Trans. Power Electron.*, vol. 30, no. 12, pp. 7159–7169, Dec. 2015.

[49] K.-T. Mok, S.-C. Tan, and S. Y. R. Hui, "Decoupled power angle and voltage control of electric springs," *IEEE Trans. Power Electron.*, vol. 31, no. 2, pp. 1216–1229, Feb. 2016.

[50] S. Yan, M.-H. Wang, J. Chen, and S. Y. Hui, "Smart loads for improving the fault-ride-through capability of fixed-speed wind generators in microgrids," *IEEE Trans. Smart Grid*, vol. 10, no. 1, pp. 661–669, Jan. 2019.

[51] S. Yan, M.-H. Wang, T.-B. Yang, S.-C. Tan, B. Chaudhuri, and S. Y. R. Hui, "Achieving multiple functions of three-phase electric springs in unbalanced three-phase power systems using the instantaneous power theory," *IEEE Trans. Power Electron.*, vol. 33, no. 7, pp. 5784–5795, Jul. 2018.

[52] C. K. Lee, N. R. Chaudhuri, B. Chaudhuri, and S. Y. R. Hui, "Droop control of distributed electric springs for stabilizing future power grid," *IEEE Trans. Smart Grid*, vol. 4, no. 3, pp. 1558–1566, Sep. 2013.

[53] X. Chen, Y. Hou, and S. Y. R. Hui, "Distributed control of multiple electric springs for voltage control in microgrid," *IEEE Trans. Smart Grid*, vol. 8, no. 3, pp. 1350–1359, May 2017.

[54] M.-H. Wang, S. Yan, S.-C. Tan, Z. Xu, and S. Y. Hui, "Decentralized control of DC electric springs for storage reduction in DC microgrids," *IEEE Trans. Power Electron.*, vol. 35, no. 5, pp. 4634–4646, May 2020.

[55] X. Chen, M. Shi, H. Sun, Y. Li, and H. He, "Distributed cooperative control and stability analysis of multiple DC electric springs in a DC microgrid," *IEEE Trans. Ind. Electron.*, vol. 65, no. 7, pp. 5611–5622, Jul. 2018.

[56] J. Liao, N. Zhou, Y. Huang, and Q. Wang, "Unbalanced voltage suppression in a bipolar DC distribution network based on DC electric springs," *IEEE Trans. Smart Grid*, vol. 11, no. 2, pp. 1667–1678, Mar. 2020.

MINGHAO WANG (Member, IEEE) received the B.Eng. degree (Hons.) from the Huazhong University of Science and Technology, Wuhan, China, and the University of Birmingham, Birmingham, U.K., in 2012, and the M.Sc. and Ph.D. degrees in electrical and electronic engineering from the University of Hong Kong, Hong Kong, in 2013 and 2017, respectively. Since 2018, he has been with the Department of Electrical Engineering, The Hong Kong Polytechnic University. He is currently a Research Assistant Professor. His research interests include smart grid technologies, ac–dc power conversion, power systems, electric springs, and power electronics.

YUFEI HE (Member, IEEE) received the B.Eng. degree in electronic and information engineering from Zhejiang University, Hangzhou, China, in 2016, and the Ph.D. degree in electrical engineering from The Hong Kong Polytechnic University, Hong Kong, China, in 2020. He is currently a Postdoctoral Research Fellow with the Department of Electrical Engineering, The Hong Kong Polytechnic University. His research interest includes power electronic control for grid-integration of renewables.

XU XU (Member, IEEE) received the M.E. and Ph.D. degrees from The Hong Kong Polytechnic University, Hong Kong, SAR, in 2016 and 2019, respectively. He is currently with the Department of Electrical Engineering, The Hong Kong Polytechnic University. He is also with the School of Electrical and Electronic Engineering, Nanyang Technological University, Singapore. His current research interests include power system planning and operation, renewable power integration, energy management, and artificial intelligence application in power engineering.

ZHEKANG DONG (Member, IEEE) received the B.E. and M.E. degrees in electronics and information engineering from Southwest University, Chongqing, China, in 2012 and 2015, respectively, and the Ph.D. degree from the School of Electrical Engineering, Zhejiang University, China, in 2019. He is currently an Associate Professor with Hangzhou Dianzi University, Hangzhou, China. He is also a Research Assistant with The Hong Kong Polytechnic University. His research interests include nonlinear circuit, memristor theory, and neural networks.

YU LEI received the B.S. degree in electrical engineering and automation from the Huazhong University of Science and Technology and the University of Birmingham, in 2012, and the M.S. degree in control system from the Imperial University of Technology, in 2013. She is currently working with the School of Automation, Wuhan University of Technology. As a Lecturer, she has participated in a number of three-dimensional measurement projects. Her major research interests include intelligent control and pattern recognition.